ELSEVIER

Journal of Magnetism and Magnetic Materials 249 (2002) 234–240

journal of magnetism and magnetic materials

www.elsevier.com/locate/jmmm

High density hexagonal nickel nanowire array

K. Nielsch[a,*], R.B. Wehrspohn[a], J. Barthel[a], J. Kirschner[a], S.F. Fischer[b], H. Kronmüller[b], T. Schweinböck[c], D. Weiss[c], U. Gösele[a]

[a] *Max-Planck-Institute of Microstructure Physics, Weinberg 2, 06120 Halle, Germany*
[b] *Max-Planck-Institute of Metal Research, Heisenbergstr. 1, 70569 Stuttgart, Germany*
[c] *Institute of Applied Physics, University of Regensburg, 93040 Regensburg, Germany*

Abstract

Nickel nanowires were grown in highly ordered pore channels of an alumina membrane using pulsed electrodeposition. A complete metal filling of the hexagonal arranged pores with a pitch of 100 nm and a monodisperse pore diameter of ≈ 30 nm was obtained. The bulk-magnetic behavior of the ferromagnetic nanowire arrays was characterized by SQUID-magnetometer measurements. Magnetic-force-microscopy investigation measurements with a variable external magnetic field were applied on magnetized and demagnetized samples. In addition, magnetic wires have been locally switched by a strong MFM tip and an external magnetic field. The MFM results show a good agreement with the bulk magnetic hysteresis loop.

Keywords: Nanowires; Nickel; Magnetic dipolar interactions; Porous alumina; Magnetic force microscope

1. Introduction

The application of ferromagnetic-material-filled ordered matrices for perpendicular magnetic storage media is becoming increasingly relevant to extend the areal density of magnetic storage media beyond the predicted superparamagnetic limit ($>70\,\mathrm{Gbit/in^2}$) [1,2]. One bit of information corresponds to one single-domain nanosized particle or the so-called nanomagnet. Since each bit would be composed of a single large aspect particle, the areal density of pattered media can, in principle, be much more than an order of magnitude higher than in conventional longitudinal media. For example, an areal density of about $300\,\mathrm{Gbit/in^2}$ can be achieved by a hexagonal arranged array of nanomagnets with a lattice constant of about 50 nm.

The fabrication of nanomagnet arrays based on hexagonal arranged porous alumina as a template material is cheaper than that based on traditional fabrication methods like nanoscaling using electron-beam lithography [3]. Moreover, these arrays of magnetic nanowires can be easily fabricated over areas of several $\mathrm{cm^2}$. Since 1981, several articles on unarranged porous alumina templates filled with ferromagnetic materials have been published [4–8]. These structures have large size distributions of the pore diameter and inter-pore distance and the filling degree of the pores is not specified. Based on an approach by Masuda [9], we have shown that ordered porous alumina arrays with a sharply defined pore diameter and

*Corresponding author.
E-mail address: elch@mpi-halle.de (K. Nielsch).

0304-8853/02/$ - see front matter
PII: S0304-8853(02)00536-X

inter-pore distance can be obtained by a two-step electrochemical anodization process of aluminium [10,11]. The degree of self-ordering is polydomain with a typical domain size of a few microns. Monodomain pore arrays can be obtained by electron-beam lithography [12] or imprint technology [13].

2. Magnetic structure

The magnetic structure characterized in this work is a highly ordered nickel nanowire array which is embedded in an alumina matrix and fixed to a silicon substrate (Fig. 1a). The magnetic columns are arranged in a hexagonal pattern with a wire-to-wire distance $D_{\mathrm{int}} = 100\,\mathrm{nm}$, which corresponds to a density of the anisotropic particles of $C = 11.6 \times 10^{13}\,\mathrm{m}^{-2} \approx 75 \times 10^{9}\,\mathrm{in}^{-2}$. The pillars have a diameter of about $D_{\mathrm{P}} = 30\,\mathrm{nm}$, with a standard deviation of less than 10%, a length of about $L = 700\,\mathrm{nm}$ and are extended over the whole thickness of the oxide matrix. The magnetic pillars were grown by a pulsed electrochemical deposition process in a highly ordered porous oxide template. The fabrication of these highly ordered porous alumina template filled with ferromagnetic materials was recently reported in detail by us in Ref. [14]. Additional information on the preparation of this structure for the magnetic characterization is given in Ref. [15].

As an example, Fig. 1b shows an SEM image of the nickel sample. The ferromagnetic nanowires (white) with a monodisperse diameter are embedded in the porous alumina matrix (black). Due to the self-organization process, the nanowires are arranged in a hexagonal pattern. All nanowires are visible at the matrix surface and 100% pore filling was obtained for all samples discussed in this work. The metallic pillars are nano-crystalline and their average grain size ranges from 10 to 15 nm, see Ref. [14].

3. Magnetic properties and discussion

The bulk magnetic properties of the highly ordered array with high-aspect ratio magnetic

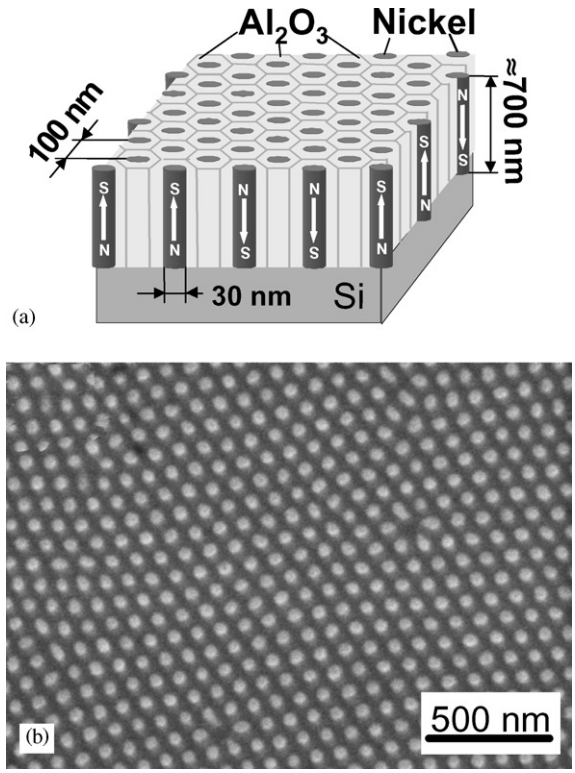

Fig. 1. (a) Sketch of the magnetic structure. Nickel nanowires are arranged in a hexagonal array perpendicular to a silicon substrate and embedded in an aluminium oxide matrix. (b) Top-view SEM micrograph of a nickel-filled alumina matrix with an inter-pore distance of 100 nm fixed on a silicon substrate. The Ni columns have a diameter $D_{\mathrm{P}} = 30\,\mathrm{nm}$ and a length of $\sim 700\,\mathrm{nm}$.

columns (length/diameter ~ 25) were investigated by SQUID-magnetometer measurements. Fig. 2 shows the bulk magnetization hysteresis loops for the nickel array measured with an applied field parallel and perpendicular to the wire axis.

The hysteresis loops measured for the nickel nanowire (Fig. 2) array with the magnetic field applied parallel to the wire axis show a coercive field of $H_{\mathrm{C}}^{\parallel} = 1200\,\mathrm{Oe}$ and a squareness of nearly 100%. The measured coercive fields for the hysteresis loops measured perpendicular to the wire are $H_{\mathrm{C}}^{\perp} \approx 150\,\mathrm{Oe}$ and drastically smaller than $H_{\mathrm{C}}^{\parallel}$. This sample has a preferential magnetic orientation along the wire axis. Here, we give only a short description of the analysis of the sample. A

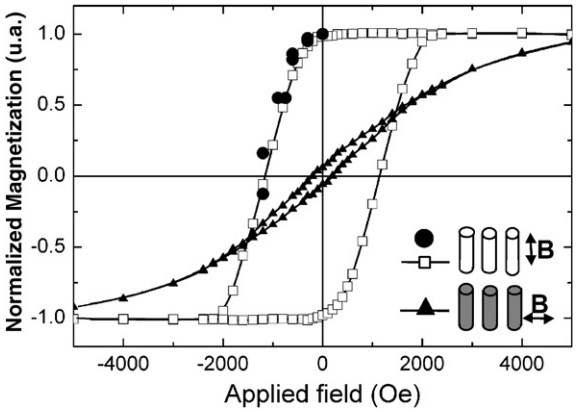

Fig. 2. SQUID-hysteresis loops of the nickel nanowire array with a pitch of 100 nm, column length of about 700 nm and a wire diameter of 30 nm measured with an applied field parallel (□) and perpendicular (▲) to the column axis. Results from MFM investigations (●) while an external magnetic field H_{ex} was applied to the sample (analyzed statistically treated).

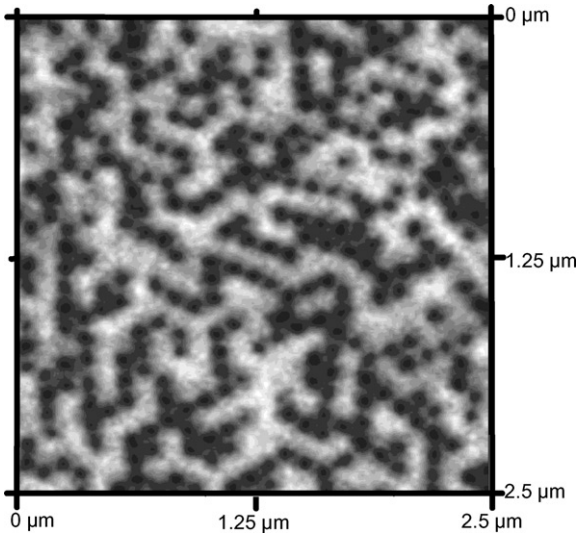

Fig. 3. Magnetic-force-microscopic image of the highly ordered nickel nanowire array with a pitch of 100 nm embedded in the alumina matrix in the demagnetized state, showing the magnetic polarization of the pillars alternately "up" (white) and "down" (black).

detailed analysis about influence of the nanowire diameter on the bulk-magnetic properties of hexagonally ordered 100 nm period nickel nanowire arrays can be found in Ref. [16]. The total magnetic anisotropy of this sample is influenced by the magnetic anisotropy resulting from the shape of the Ni nanowires ($H_S = 2\pi M_S = 3200$ Oe) and the dipole or the so-called demagnetization fields ($H_D^{\parallel} = \pi^2 M_S D_P^2 c \approx 550$ Oe; c: pore density) between the nanowires. The magneto-crystalline anisotropy of the nano-crystalline Ni wires gives only a small contribution ($H_K = 2K_1/M_S = 195$ Oe) at room temperature. The Ni nanomagnets are single domain particles. Their magnetic reversal process occurs by inhomogeneous switching modes, as confirmed by micromagnetic modeling [17]. The small size distribution of the pore diameter ($\Delta D_P/D_P < 10\%$) [9,11] has a positive impact on the magnetic properties. Here, we report the highest measured coercive fields H_C of about 1200 Oe for a close-packed nickel nanowire array embedded in a membrane matrix. Previous works on unarranged nickel nanowire arrays show lower coercive fields of about 1000 Oe or less in the preferential magnetic orientation [8,18]. The large size distribution (up to $\Delta D_P/D_P > 50\%$) [7] of the pore diameters and the inter-wire distance enhance the magnetic interactions in the nanowire arrays and reduce the squareness of the hysteresis loop.

In contrast, the MFM images reflect the magnetic polarization at the top end of each magnetic nanowire. Fig. 3 demonstrates the domain structure of an array of nickel columns in the demagnetized state. The geometric parameters of the sample are the same as for Fig. 1b. Dark spots in the magnetic image imply the magnetization pointing up and bright spots imply the magnetization pointing down. Up magnetization may be interpreted as a binary '1' and down magnetization as a binary '0'. It can be deduced from the picture that the Ni pillars are single domain nanomagnets aligned perpendicular to the surface. The patterned domain structure is due to an antiferromagnetic alignment of pillars influenced by the weak magnetic interaction between these nanomagnets. The labyrinth pattern (Fig. 3) of the domain structure is characteristic for hexagonally arranged single-domain magnetic particles with a perpendicular magnetic orientation in the demagnetized state. In the case of a quadratic lattice,

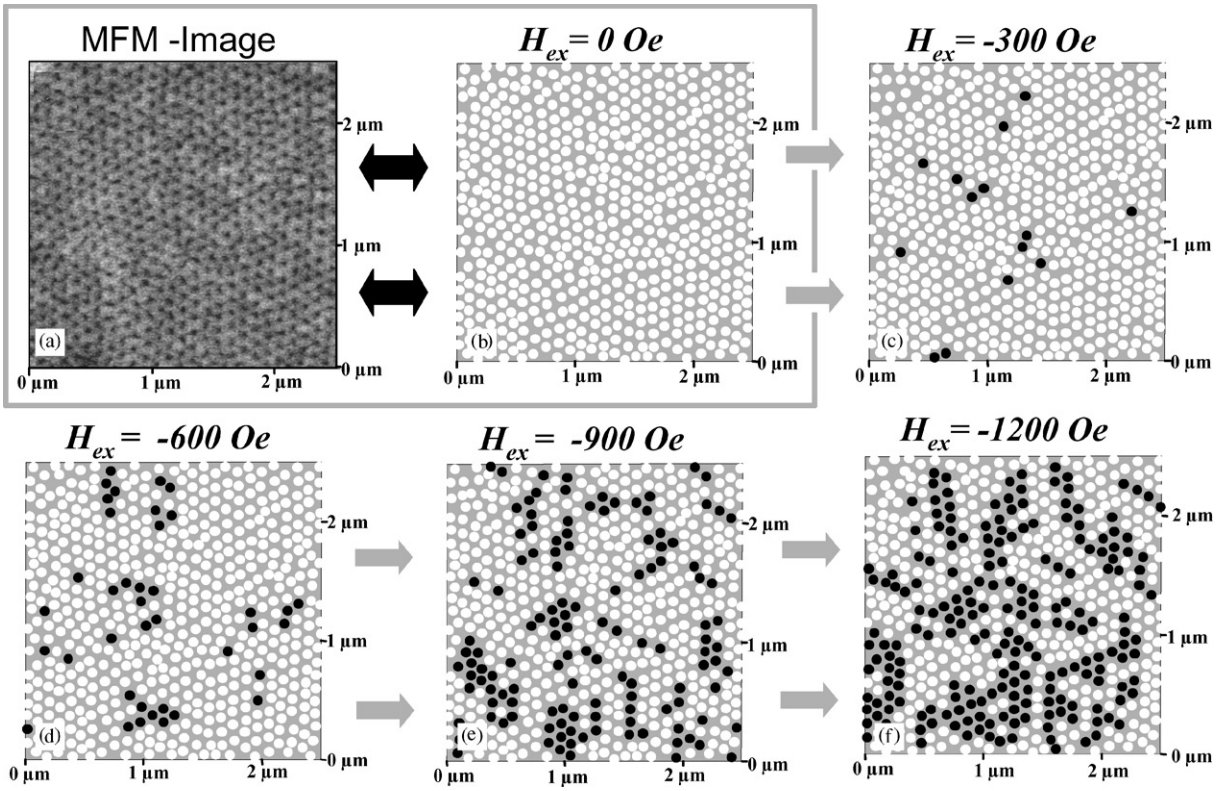

Fig. 4. An external magnetic field was applied perpendicular to the sample surface. (a) The MFM image of the completely magnetized nanowire array. The MFM image (a) was enhanced numerically (a and b). Numerically enhanced MFM images recorded with an applied magnetic field of $H_{ex} = -300$ (c), -600 (d), -900 (e) and -1200 Oe (f).

each of the four nearest-neighbors will be aligned antiparallel and the domain structure exhibits a checkerboard pattern [2]. In the hexagonal lattice, two of the six nearest-neighbors will align their magnetization parallel and four will be magnetized anti-parallel, if the stray field has only nearest-neighbor interaction. In Fig. 3, we observe that in average 2.5 nanomagnets are aligned parallel and that 3.5 are magnetized antiparallel. We suppose that the stray field interaction is extended over several lattice periods D_{int}, due to the high aspect ratio of the magnetic nanowire.

Additionally, MFM investigations with applied magnetic field were carried out on the sample to study the switching behavior of the individual nanowires in the array. A low moment magnetic tip was used for the MFM scan, in order to prevent switching of the magnetization in the nanowires by the dipole field of the magnetic tip ($H_{tip} \approx 50$ Oe). Before this investigation, the sample was completely magnetized by an external magnetic field of about 5000 Oe along the wire axes. The first scan was perform without an external field, see Fig. 4a. In order to get a better impression about the magnetic polarization of each pillar, the MFM images were numerically enhanced (Fig. 4a and b). There are no differences in the magnetic polarization between the magnetic pillars (Fig. 4a) and in the enhanced image every nanowire shows a positive polarization (white dots). Due to the fact that the applied field H_{ex} was larger than the saturation field $H_S^{\parallel}$ and that the hysteresis loop has a magnetic squareness of about 100%, we may deduce that the magnetization in each pillar of the array is oriented in one direction (up or down). Even though $H_{ex} = 0$ Oe and the

maximum demagnetization field of $H_D = -550$ Oe is achieved, the structure remains in the saturated state. During the following MFM scans an increased external magnetic field is applied in the direction opposite to the magnetization. The numerically enhanced images are shown for $H_{ex} = -300$ Oe (Fig. 4c), -600 Oe (Fig. 4d), $H_{ex} = -900$ Oe (Fig. 4e) and $H_{ex} = -1200$ Oe (Fig. 4f). When the external field is increased, the effective field in the sample increases: $H_{eff} = H_D + H_{ex}$. In Fig. 4c an average effective field of about 850 Oe is obtained. Due to fluctuations of the local dipole fields and the switching fields of the individual nanowires, a few magnetic particles reverse their magnetization (black dots) also in the case $H_{eff} < H_C^{\parallel}$. Increasing the external field leads to an increasing number of reversed magnetized pillars (Fig. 4b–f). The enhancement of H_{eff} is partly compensated by the reduced dipole interactions from the reversed pillars. In the final image (Fig. 4f) the applied external field has reached the coercive field $H_C^{\parallel} = 1200$ Oe. The number of switched (black) and unswitched (white) nanowires are nearly equal. In this case, the average demagnetization field in the sample will be reduced nearly to a minimum and $H_{ex} \approx H_{eff} \approx H_C^{\parallel}$. Additionally, our MFM images were statistically analyzed and compared with the data from the measured hysteresis loop in the preferential magnetic orientation, see Fig. 2 ($H_{ex} \parallel$ wire). With a few fluctuations the MFM analysis corresponds very well to the bulk magnetic characterization of the sample.

In order to examine in more detail the suitability of this nickel nanowire array for patterned perpendicular magnetic media, we have tried to completely magnetized a defined area of a demagnetized sample by a strong magnetic MFM tip ($H_{Tip} \approx 250$ Oe) and an external magnetic field ($H_{ex} = -1200$ Oe). The amount of the applied external field was nearly equal to the average switching field (H_{sw}) of the individual nanowire ($H_{sw} \approx H_C^{\parallel} = 1200$ Oe) and was applied in the direction of the nanowire axis. Starting in the upper region of Fig. 5 the strong magnetic tip was scanned over an area of $5 \times 5\ \mu m^2$. Hereby, a total external field of about $H'_{ex} = H_{ex} + H_{Tip} = -1450$ Oe was applied locally to the tips of the nickel nanowires. Subsequently, the external magnetic field was switched off. An

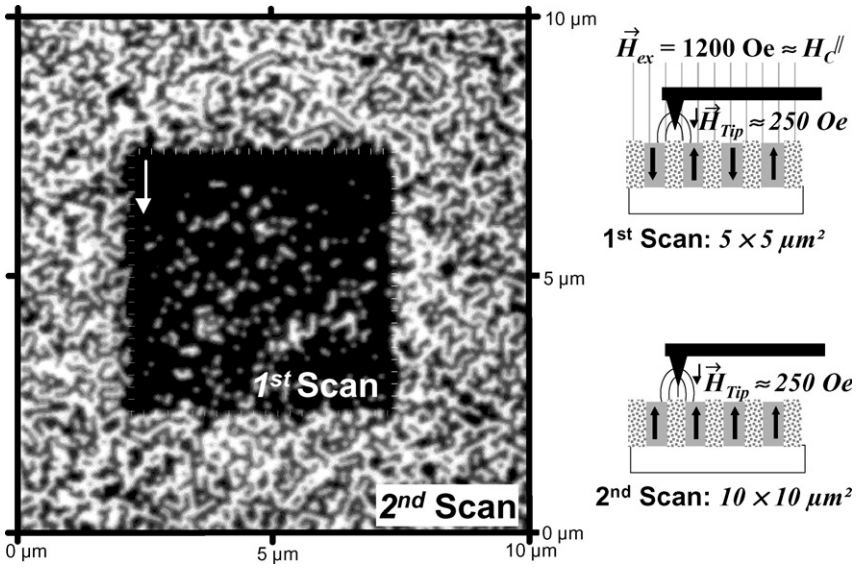

Fig. 5. Local magnetic switching of a demagnetized sample area ($5 \times 5\ \mu m^2$, 1st scan) by a strong magnetic MFM tip ($H_{Tip} \approx 250$ Oe) and an external magnetic field ($H_{ex} = -1200$ Oe). This image of the domain pattern ($10 \times 10\ \mu m^2$) was recorded by a second subsequent MFM scan without an external magnetic field.

enlarged area of $10 \times 10\,\mu m^2$ (Fig. 5) was scanned with the magnetic tip in order to measure the domain pattern of the manipulated area in the nanowire array. Inside the area of the first scan nearly every nickel column ($\sim 93\%$) is magnetized in the same direction.

Fig. 5 shows the local impact (dark quadratic region) of the external magnetic field and the strong magnetic tip during the first MFM scan on the magnetization of nanowires. Around the magnetized region of $5 \times 5\,\mu m$, the nickel nanowire array remained in the demagnetized state and exhibited the labyrinth-like domain pattern (Fig. 3). The border between the magnetized area and the surrounding demagnetized area is clearly visible. From the picture, it can be concluded that applied magnetic field ($H_{sw} \approx H_C^{\parallel}$) alone was not strong enough for the switching of magnetic polarization in the Ni columns. Hence, the additional field contribution form the strong MFM tip (H_{Tip}) enabled the local switching process in the Ni nanowire array.

The probability for a nickel nanowire to remain unswitched (light spots) increases in the lower region of the magnetically manipulated area (Fig. 5: 1st scan). In the upper region, where the first magnetic scan procedure had started, the first five or six horizontal nanowire rows have been completely magnetized in the same direction. During the first scan procedure when the area of the completely magnetized nanowires was growing, the probability for nanomagnet to remain unswitched increased. We assume that the stray-field interactions between the demagnetized and the magnetized area can be neglected and the net strayfield in the demagnetized area is zero. By increasing the area of parallel magnetized nanowires the dipole interactions between the magnetic elements are enhanced and the applied local field ($H_{Tip} + H_{ex}$) is getting less sufficient for a complete magnetic alignment of magnetization in a horizontal row of nickel columns. At the left and right border of the magnetically manipulated area, the strayfield interactions are weak and a lower number of unswitched magnetic columns is observed there. From this experiment, it can be concluded that the strayfield dipole interactions between the nanowires are extended over several inter-wire distances due to their high aspect ratio (nanowire length to inter-wire distance: $L/D_{int} \approx 7$). In principle, the single nanowire can store one bit of information and can be locally switched independently to the magnetization of its nearest neighbors.

4. Conclusion

The measurement of the bulk-magnetic properties shows a strong magnetic anisotropy along the nickel column axes, coercive fields of 1200 Oe and nearly 100% squareness. In the demagnetized state, the nanowire array exhibits a labyrinth-like domain pattern. Good agreement between the MFM investigation in the presence of an external magnetic field and the hysteresis loop was obtained. Each magnetic pillar is a single-domain magnetic particle, magnetized perpendicular to the template surface and, in principle, can store one bit of information.

References

[1] R. O'Barr, S.Y. Yamamoto, S. Schultz, W. Xu, A. Scherer, J. Appl. Phys. 81 (1997) 4730.
[2] C.A. Ross, H.I. Smith, T.A. Savas, M. Schattenberg, M. Farhoud, M. Hwang, M. Walsh, M.C. Abraham, R.J. Ram, J. Vac. Sci. Technol. B 17 (1999) 3159.
[3] D. Routkevitch, A.A. Tager, J. Haruyama, D. Almawlawi, M. Moskovits, J.M. Xu, IEEE Trans. Electron. Dev. 147 (1996) 1646.
[4] M.P. Kaneko, IEEE Trans. Magn. MAG-17 (1981) 1468.
[5] D. AlMawlawi, N. Coombs, M. Moskovits, J. Appl. Phys. 69 (1991) 5150.
[6] L. Feiyue, R.M. Metzger, W.D. Doyle, IEEE Trans. Magn. 33 (1997) 3715.
[7] G.J. Strijkers, J.H.J. Dalderop, M.A.A. Broeksteeg, H.J.M. Swagten, W.J.M. de Jonge, J. Appl. Phys. 86 (1999) 5141.
[8] H. Zeng, M. Zheng, R. Skomski, D.J. Sellmyer, Y. Liu, L. Menon, S. Bandyopadhyay, J. Appl. Phys. 87 (2000) 4718.
[9] H. Masuda, K. Fukuda, Science 268 (1995) 1466.
[10] A.-P. Li, F. Müller, A. Birner, K. Nielsch, U. Gösele, J. Appl. Phys. 84 (1998) 6023.
[11] R.B. Wehrspohn, A.P. Li, K. Nielsch, F. Müller, W. Erfurth, U. Gösele, The Electrochemical Society Proceedings Series, PV 2000-4, Pennington, NJ, 2000, p. 271.
[12] A.P. Li, F. Müller, U. Gösele, Electrochem. Soc. Lett. 3 (2000) 131.

[13] H. Masuda, H. Yamada, M. Satoh, H. Asoh, M. Nakao, T. Tamamura, Appl. Phys. Lett. 71 (1997) 2770.
[14] K. Nielsch, F. Müller, A.P. Li, U. Gösele, Adv. Mater. 12 (2000) 582.
[15] K. Nielsch, R.B. Wehrspohn, S.F. Fischer, H. Kronmüller, J. Barthel, J. Kirschner, U. Gösele, MRS Symp. Proc. 636 (2001) D1.9.1.
[16] K. Nielsch, R. Wehrspohn, J. Barthel, J. Kirschner, U. Gösele, S.F. Fischer, H. Kronmüller, Appl. Phys. Lett. 79 (2001) 1360.
[17] K. Ounadjela, R. Ferré, L. Louail, J.M. George, J.L. Maurice, L. Piraux, S. Dubois, J. Appl. Phys. 81 (1997) 5455.
[18] H.B. Braun, J. Appl. Phys. 85 (1999) 6172.